



Cite this: *J. Anal. At. Spectrom.*, 2020, **35**, 320

# Precise measurement of selenium isotopes by HG-MC-ICPMS using a 76–78 double-spike†

Marie-Laure Pons,<sup>a</sup> \*<sup>ab</sup> Marc-Alban Millet,<sup>c</sup> Geoff N. Nowell,<sup>d</sup> Sambuddha Misra<sup>ae</sup> and Helen M. Williams<sup>a</sup>

Selenium (Se) stable isotopes are a new geochemical tool with great potential as a tracer of redox processes and chemical cycling of chalcophiles and volatile elements. However, Se isotope measurements in low-Se samples present a formidable analytical challenge. In this study, we report a new method to measure Se stable isotopes ( $\delta^{82/78}\text{Se}$ ; per mil deviation relative to Se NIST SRM 3149) with extremely high precision. Selenium has six stable isotopes and therefore is a good candidate for isotope analysis using a double spike approach, which has the advantage that it can correct for any stable isotope fractionation that may occur during sample processing. We have calibrated a novel  $^{76}\text{Se}$ – $^{78}\text{Se}$  double spike and have developed a rapid and precise analytical protocol on a multi-collector inductively coupled plasma mass spectrometer using an ESI hydride generation introduction system. Sensitivity is over 1000 V per ppm for the total Se signal; a measurement typically requires 25 ng of natural Se. Argon dimer interferences on masses 76, 78 and 80 were corrected *in situ* by measuring mass 80. Germanium interferences on masses 74 and 76 were corrected by measuring mass 73 and mass 75 was monitored to correct for arsenic hydride on mass 76. Wash-out times were in the order of 180 s, greatly reduced compared to previous studies that rely on on peak zero argon dimer corrections (wash-out times of up to one hour). The 2 s.e. error for a single analysis typically ranges from 0.01 to 0.025‰ ( $n = 80$ ) for  $\delta^{82/78}\text{Se}$ . Long-term reproducibility and accuracy were estimated by multiple analyses of the Se Merck standard over numerous different analytical sessions, resulting in a mean  $\delta^{82/78}\text{Se}$  value of  $-0.989 \pm 0.034\%$  ( $n = 93$ ; 2 s.d.), which is in excellent agreement with previous studies.

Received 1st October 2019  
 Accepted 2nd December 2019

DOI: 10.1039/c9ja00331b

rsc.li/jaas

## 1. Introduction

Recent progress in plasma source multi-collector mass spectrometry in the last few decades has enabled the development of techniques for the measurement of previously unexplored isotope systems, the so-called “non-traditional” elements, including magnesium, iron, titanium, molybdenum, chromium and selenium.<sup>1–6</sup> Selenium (Se) has six stable isotopes ( $^{74}\text{Se}$ , 0.889%;  $^{76}\text{Se}$ , 9.366%;  $^{77}\text{Se}$ , 7.635%;  $^{78}\text{Se}$ , 23.772%;  $^{80}\text{Se}$ , 49.607% and  $^{82}\text{Se}$ , 8.731%), displays a similar chemical behaviour to sulphur, and exhibits multiple redox states, from reduced Se(–II) to the most oxidized Se(VI). For these reasons, Se stable isotopes have received considerable attention from the

geochemistry community. For example, previous studies have demonstrated that Se stable isotopes have the potential to constrain the redox evolution of the Earth’s ocean and atmosphere through time using sulphide and Se-rich sedimentary records,<sup>7–14</sup> and Se isotopes have also been used to constrain redox processes and biogeochemical cycling in the critical zone.<sup>15–20</sup>

However, the Se isotope compositions of the Earth’s mantle and other major chemical reservoirs remain poorly constrained,<sup>21–25</sup> limiting further application of this system to terrestrial and planetary geology. This is in part due to the very low abundances of Se in mantle rocks (typically 3–100 ppb (ref. 26–28)) coupled with multiple analytical challenges, such as the low ionisation efficiency of Se in argon plasmas and multiple interferences from argide species as well as germanium and arsenic, which are present at significant concentrations in target samples. A number of different analytical strategies have been employed to deal with these challenges, all of which have their own inherent advantages and disadvantages.<sup>6,29–35</sup> Here we present a method allowing measurements of Se stable isotopes ( $\delta^{82/78}\text{Se}$ ; per mil deviation relative to Se NIST SRM 3149) in geological samples with increased precision. We have employed a double spike approach, as previous studies have

<sup>a</sup>The University of Cambridge, Department of Earth Sciences, Downing St, Cambridge CB2 3EQ, UK. E-mail: dr.marie.laure.pons@gmail.com

<sup>b</sup>CNRS, Aix Marseille Univ, IRD, INRA, Coll France, CEREGE, 13545, Aix en Provence, France

<sup>c</sup>Cardiff University, School of Earth and Ocean Sciences, Main Building, Park Pl, Cardiff CF10 3AT, UK

<sup>d</sup>Durham University, Department of Earth Sciences, Elvet Hill, Durham DH1 3LE, UK

<sup>e</sup>Indian Institute of Science, Centre for Earth Sciences, Bengaluru, India

† Electronic supplementary information (ESI) available. See DOI: 10.1039/c9ja00331b

demonstrated the potential of this method to yield highly accurate and precise stable isotope ratio measurements,<sup>2,36–40</sup> and focussed on the development of a new method to measure Se stable isotopes with high precision.

## 2. Double spike

Selenium stable isotope measurements are fraught with difficulty. In addition to isobaric argon-based interferences on masses 74, 76, 78 and 80, non-quantitative yields during Se purification by ion exchange chromatography and the large degree of instrumental mass bias that is inherent to plasma mass spectrometry can cause reduced precision and/or inaccuracy if not accounted for properly. The double spike method is ideally suited to generate highly precise stable isotope measurements for elements with 4 or more isotopes as it can reliably account for laboratory based stable isotope fractionation (*i.e.* the combined effects of sample processing and mass spectrometry) and also provide an exceptionally precise means of correcting for instrumental mass bias.<sup>36–42</sup> As such, it has been widely used by isotope geochemists in the development of high-precision analytical methods for a wide range of non-traditional stable isotope systems over the last decade.<sup>2,3,43–48</sup> The double spike method relies on the addition of an isotope tracer (or spike) of known composition to the sample of interest during sample processing. The final error on the stable isotope ratio is strongly dependent on the isotope composition of the spike and the mixing proportion between the sample and spike. Typically, spikes made out of a mixture of two isotopes only (*i.e.* 'double' spikes) have proven favourable over spikes made of three isotopes (*i.e.* 'triple' spikes<sup>48</sup>), provided that the composition of the 'double spike' is chosen carefully. In order to do this we modelled optimum spike compositions and spike-sample proportions for Se stable isotope measurements using the approach outlined by Millet and Dauphas in 2014,<sup>2</sup> which

takes into account the errors associated with counting statistics and collector Johnson noise (see ref. 2 for more details). Johnson noise, *i.e.* the thermal noise generated in the Faraday cup collectors, although low at room temperatures and negligible compared to counting statistics for ion beams over a few hundred millivolts, can nonetheless add a significant amount of uncertainty when low ion beams are measured. In our models we assumed that beam conditions were set as 35 V for the most abundant isotope of each mixture and all ion beams collected in collectors with  $10^{11} \Omega$  amplifiers apart from  $^{80}\text{Se}$ , where a  $10^{10} \Omega$  amplifier was employed. Room temperature was set to 25 °C and measurements consisted of 80 integrations of 4.194 s each.

Using our model approach, two potential double spikes were found to provide low errors, an  $^{82}\text{Se}$ – $^{78}\text{Se}$  spike similar to that used by Pogge *et al.* (2014)<sup>33</sup> and a  $^{76}\text{Se}$ – $^{78}\text{Se}$  double spike (Fig. 1) that allows slightly better internal precision. Both of these potential double spike solutions use  $^{76}\text{Se}$ ,  $^{77}\text{Se}$ ,  $^{78}\text{Se}$  and  $^{82}\text{Se}$  isotope signals for spike deconvolution.<sup>33</sup> The  $^{76}\text{Se}$ – $^{78}\text{Se}$  spike provides the advantage of being able to generate low analytical uncertainties over a much larger range of spike-sample mixing ratios (Fig. 1). This is particularly important in the case of low-abundance elements like Se where element concentrations may not be known with high precision prior to isotope measurements. However, a potential drawback in using this spike is that there are significant argide isobaric interferences on both  $^{76}\text{Se}$  and  $^{78}\text{Se}$  ( $^{36}\text{Ar}^{40}\text{Ar}$  and  $^{38}\text{Ar}^{38}\text{Ar}$  on mass 76;  $^{38}\text{Ar}^{40}\text{Ar}$  on mass 78, respectively) in contrast to previously used selenium double spikes such as  $^{74}\text{Se}$ – $^{77}\text{Se}$  and  $^{78}\text{Se}$ – $^{82}\text{Se}$ , which only have one interfered isotope (minor  $^{36}\text{Ar}^{38}\text{Ar}$  interference on mass 74 and significant  $^{38}\text{Ar}^{40}\text{Ar}$  interference on mass 78, respectively<sup>6,29,33,34</sup>). The presence of these argon dimer interferences requires precise interference corrections prior to spike deconvolution. In addition to argides,  $^{76}\text{Ge}$  and  $^{75}\text{AsH}$  can also interfere on mass 76, making the  $^{76}\text{Se}$  signal challenging to decipher. However, as detailed below, we can mitigate the

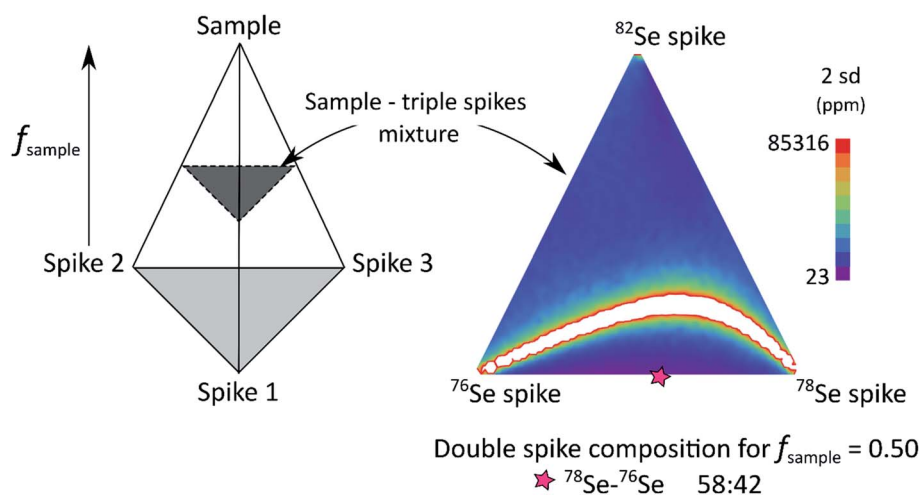


Fig. 1 Schematic representation of all the possible spike-sample mixtures investigated in our triple spike Monte-Carlo simulation. All compositions are enclosed in a tetrahedron where the top apex is the standard composition (*i.e.*, natural stable isotope composition) and base apexes (light grey area) are the individual spikes. In this tetrahedron, sections parallel to the base (represented in dark grey) contain all possible triple spike mixtures mixed with the same amount of natural sample.

effects of these interferences by developing a new protocol that allows for better correction of argon-based interferences and efficient arsenic hydride and germanium interference correction on mass 76. For these reasons, we were able to take advantage of the additional precision that a  $^{76}\text{Se}$ – $^{78}\text{Se}$  double spike can offer, with an optimal DS–sample mixture of 50 : 50. Furthermore, the use of a  $^{76}\text{Se}$ – $^{78}\text{Se}$  double spike can be advantageous in certain circumstances as it serves to boost the  $^{76}\text{Se}$  signal (also a critical isotope in  $^{82}\text{Se}$ – $^{78}\text{Se}$  double spike studies<sup>33</sup>) and therefore decrease the proportion of interfering species on a mass of interest.

### 3. Experimental

#### 3.1. Samples and reagents

All sample preparation steps, including double spike mixing, were carried out in the ultraclean part of the Arthur Holmes clean chemistry laboratory (class 1000 clean room) at Durham University, in a bespoke class 100 extraction cabinet.

**Selenium spikes.** Selenium spikes were purchased from Isoflex USA, both in elemental form. The  $^{76}\text{Se}$  spike has an enrichment level of  $99.80 \pm 0.10\%$  (certificate of analysis number 3598). The  $^{78}\text{Se}$  spike has an enrichment level of  $99.30 \pm 0.10\%$  (certificate of analysis number 3009). The  $^{76}\text{Se}$  and  $^{78}\text{Se}$  spikes were mixed in a new and cleaned PTFE Teflon bottle.

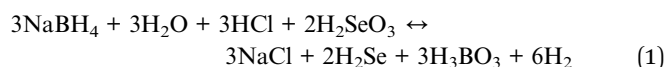
**Standards.** In this study, two selenium mono-elemental solutions with different Se isotopic compositions were used. Results were reported against a National Institute of Standards and Technology pure Se standard, NIST SRM-3149 (lot number 200901,  $10 \text{ mg g}^{-1}$ ). This single element standard solution, while not isotopically certified, is now widely used as the reference material for Se isotope measurements<sup>13,21,33,35,49,50</sup> and its absolute composition has been reported.<sup>51</sup> The second selenium standard solution used in our study is a MERCK pure Se solution which was already used as a reference by Rouxel and collaborators in their pioneering study in 2002 and was further characterised against NIST SRM-3149 by Carignan and Wen in 2007.<sup>6,35</sup> For germanium and arsenic doping experiments, mono-elemental Ge and As Specpure 1000 ppm Alpha Aesar solution were used.

**Reagents.** Distilled HCl was used to dilute the samples for Se isotope measurements and to generate hydrides (see 3.2.). Two other reagents were used in the hydride generation reaction (see eqn (1)): analytical grade sodium borohydride and extra pure sodium hydroxide pellets from Fischer Chemical.

#### 3.2. Instrumentation

**Hydride generation.** Selenium stable isotope measurements were performed with a Thermo Scientific™ Neptune Plus™ multi-collector ICP-MS coupled to an ESI HydrideICP hydride generation introduction system. We employed a hydride generator because numerous previous studies<sup>29,33,34,52</sup> have shown that Se ionises far more efficiently as a hydride, rather than in the elemental form. However, it should be noted that we measured Se isotopes on-mass as opposed to measuring the masses of Se-hydride molecular ions (which presumably break down in the plasma itself, before ionisation). The ESI hydride

generator system features a micro peripump that leads the reagents and sample through a PFA mixing block to a low-volume quartz gas–liquid separator where hydrides are formed and separated from liquid waste then carried *via* argon sample gas to the plasma torch *via* an intermediary ESI stable sample introduction dual quartz chamber, which was used to stabilise the signal. The hydrides are formed by reacting the sample, conditioned in 1 M HCl, with sodium borohydride (1 wt% NaBH<sub>4</sub> in 0.012 M NaOH) and reducing Se(IV) to Se(-II).<sup>33</sup> Prior to analysis, the sample is oxidized and conditioned in 1 M HCl. The ESI HydrideICP has three uptake lines: one for the sample, one for NaBH<sub>4</sub> and one for 1 M HCl, and solution uptake rates were adjusted on a daily basis (see Table 1). Sodium borohydride was prepared on the day of the analysis as it is known to degrade upon H<sub>2</sub> production.<sup>33</sup> The hydride generation reaction is given below:



#### MC-ICPMS operating parameters and analytical protocol.

Selenium stable isotope measurements were carried out on a Thermo Fisher Scientific™ Neptune Plus™ MC-ICPMS at the

Table 1 Operating parameters for the HG-MC-ICPMS system

Hydride generator instrument	ESI HydrideICP
<b>Solution compositions</b>	
HCl	1 N HCl
NaBH <sub>4</sub>	1 wt% NaBH <sub>4</sub> in 0.012 M NaOH
Sample/standard acidity	1 N HCl
<b>Reagent uptake rates</b>	
HCl	~0.70 mL min <sup>-1</sup> (adjusted daily)
NaBH <sub>4</sub>	~0.25 mL min <sup>-1</sup> (adjusted daily)
Sample/standard	~0.40 mL min <sup>-1</sup> (adjusted daily)
Mass spectrometry instrument	Thermo Scientific Neptune Plus
<b>MC-ICPMS cup configuration</b>	
Cup	L4 L3 L2 L1 C H1 H2 H3 H4
Mass	73 74 75 76 77 78 80 82 83
<b>MC-ICPMS material and operating parameters</b>	
Introduction system	ESI stable sample introduction dual quartz chamber
Sample cone	Nickel
Skimmer cone	Nickel
RF power	1300 W
Resolution	Low
Ar flow rates	
Cooling	~15.7 L min <sup>-1</sup> (adjusted daily)
Auxiliary	~0.8 L min <sup>-1</sup> (adjusted daily)
Sample	~1.2 L min <sup>-1</sup> (adjusted daily)
<b>Analysis</b>	
Number	1 block of 80 cycles
Integration time	4 seconds
Sample transfer time	180 seconds
Sample washout time	180 seconds

Earth Sciences Department of the University of Durham, UK. Samples were introduced through an ESI hydride generator and an ESI stable sample introduction dual quartz chamber using argon as a carrier gas. We used a regular nickel sample and skimmer cones and the analysis was carried out in low resolution mode (see Table S1† – operating parameters). The isotope ratio measurements consisted of one block of 80 integrations of 4.194 seconds each. The central cup was set on mass 77 and mass 80 was measured on the High-2 cup using a  $10^{10} \Omega$  amplifier that can accommodate a signal of up to 500 V on H2.

The samples and standards were measured in 1 M HCl after 80 seconds uptake time and the washouts were carried in 1 M HCl for 180 seconds. At the end of the washout period – and before any sample or standard measurement – an on peak zero (OPZ) of 1 block (10 integrations of 4.194 seconds each) was performed in clean 1 M HCl. All samples were bracketed with measurements of standards that were spiked and treated similarly to the samples, with concentrations and spike Se : natural Se concentration ratios carefully matched in order to account for variation in the intensity of residual

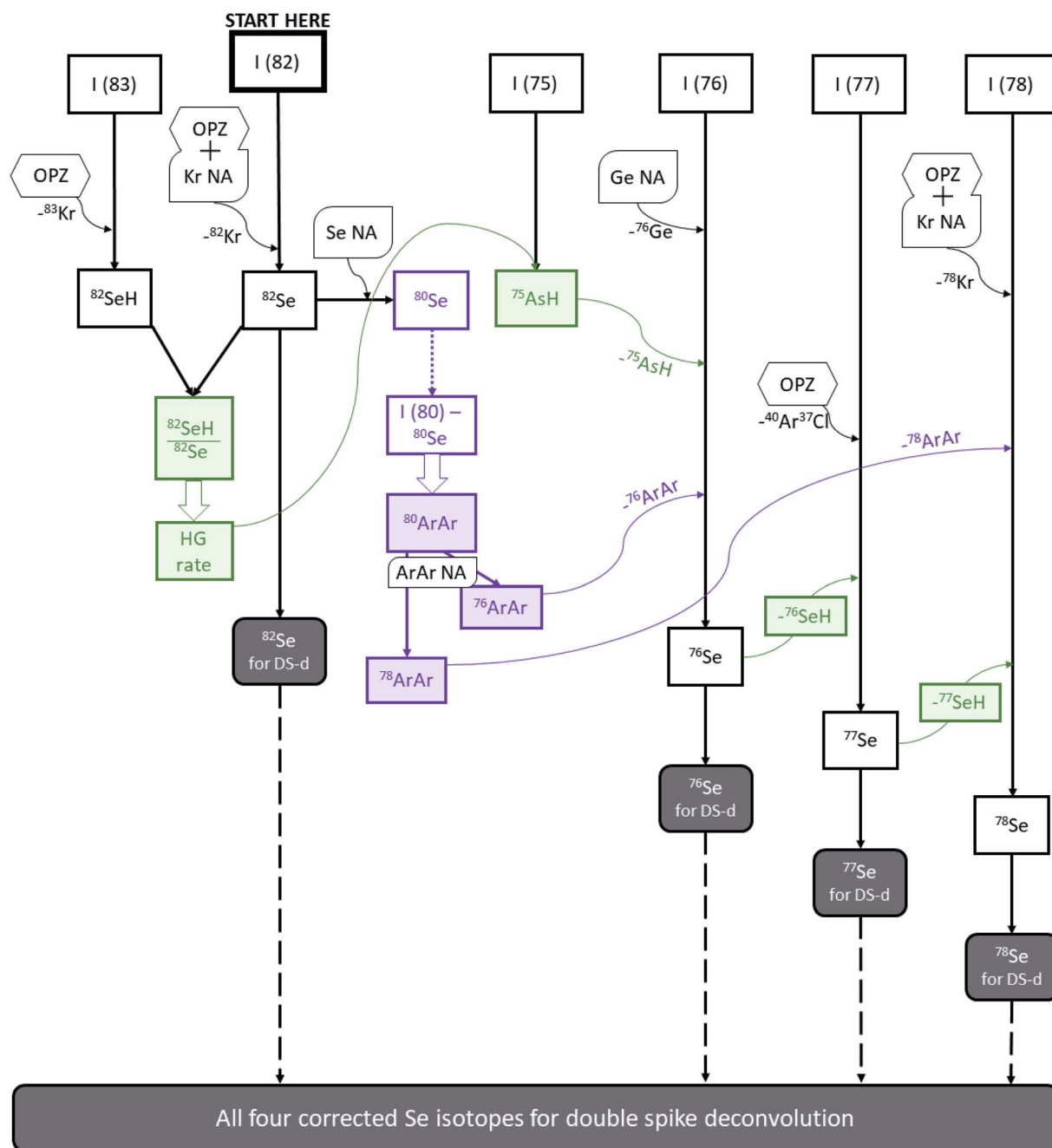


Fig. 2 Flowchart illustrating the corrections done to the intensities on masses 76, 77, 78 and 82 to extract the real selenium signal from all the isobaric interferences prior to double spike deconvolution, as described in paragraph 4. OPZ: on peak zero. NA: natural abundance. HG rate: hydride generation rate. DS-d: double spike deconvolution. In green: hydride correction. In purple: argon dimer correction.

interferences. The overall Se sensitivity in low resolution mode using the ESI HydrideICP is 1000 V per ppm (total Se beam) on average. All the data reported in this paper – unless stated otherwise – were obtained for a sample and standard concentration of 50 ppb, which gives a signal of ~2–2.4 V on mass 82. The multiple interference corrections used in this study are described below. All measurements are reported in the  $\delta$  notation as relative per mil difference to the international Se standard NIST SRM 3149 as follows:

$$\delta^{82/78}\text{Se}_{\text{sample}} = \left[ \left( \frac{^{82/78}\text{Se}_{\text{sample}}}{^{82/78}\text{Se}_{\text{NIST-SRM-3149}}} - 1 \right) \times 1000 \right] \quad (2)$$

Critically, the use of a double spike does not preclude the presentation of data in terms of stable isotope ratios employing a “spiked” isotope as the entire premise of using a double spike relies on mass dependent fractionation as applied to all measured isotopes used in the double spike deconvolution.<sup>3,48</sup>

### 3.3. Interference correction

The measurements of Se isotope ratios represents an enormous technical challenge, as all of the selenium isotopes present isobaric interferences from other elements (*e.g.* germanium) and polyatomic interferences from molecular compounds (*e.g.* argon dimers and Se hydrides). These interferences must be corrected prior to double-spike deconvolution, as shown in the isobaric interference correction flowchart (Fig. 2). The interferences on Se isotopes are also summarized in Table 2, along with the correction method used in this study, for each of them.

**Argon dimer corrections.** Argon dimer isobaric interferences constitute a technical challenge for the measurement of selenium isotopic ratios by plasma source mass spectrometry. Depending on the argon isotopes involved, argon dimers interfere with selenium isotopes at  $m/z$  ratios of 74 ( $^{38}\text{Ar}^{36}\text{Ar}^+$ ), 76 ( $^{38}\text{Ar}^{38}\text{Ar}^+$ ,  $^{40}\text{Ar}^{36}\text{Ar}^+$ ), 78 ( $^{40}\text{Ar}^{38}\text{Ar}^+$ ) and, mostly, 80 ( $^{40}\text{Ar}^{40}\text{Ar}^+$ ). The argide production depends on plasma energy fluctuation and the mass spectrometer tuning parameters. For a Se isotope measurement at 50 ppb Se, with the operating parameters as described as in Table 1, the contribution of  $^{40}\text{Ar}^{40}\text{Ar}^+$  dimers at  $m/z = 80$  is typically ~13 to 20 V on H2, while the contribution of  $^{80}\text{Se}^+$  is typically ~25 V on H2. Due to plasma instability, we found that using a background on-peak zero

(OPZ) correction to correct for ArAr interferences on masses 76, 78 and 80, used in the double spike deconvolution, generated significant errors of up to 1‰ on the  $\delta^{82/78}\text{Se}$  of the samples. Consequently, we developed an alternative approach to correct for argon dimers at every integration during the measurement, broadly following the methods of Elwaer and Hintelmann (2008)<sup>53</sup> and Stüeken *et al.*, 2013,<sup>34</sup> which account for plasma instabilities during the run. Given the IUPAC recommended values for natural abundances of  $^{82}\text{Se}$  and  $^{80}\text{Se}$ ,<sup>54</sup> we used the  $^{82}\text{Se}$  beam to predict the contribution of  $^{80}\text{Se}$  to the signal measured at  $m/z = 80$  (Fig. 2, purple path). In our method, there are no Se isotopes without background interferences, but among them,  $^{82}\text{Se}$  requires the least interference correction, hence its use in our Ar dimer correction. The contribution of  $^{80}\text{Se}$  at  $m/z = 80$  is thus

$$^{80}\text{Se} = ^{82}\text{Se}_{\text{corr}} \frac{49.80}{8.82} \quad (3)$$

with  $^{82}\text{Se}_{\text{corr}}$  being  $^{82}\text{Se}$  corrected for  $^{82}\text{Kr}$  using an on-peak zero subtraction for background Kr. During the OPZ performed at the end of the washout,  $^{83}\text{Kr}$  is measured on mass 83. Using the measured  $^{83}\text{Kr}$  and Kr natural abundance,<sup>54</sup> the  $^{82}\text{Kr}$  signal in the OPZ is calculated. This value is then subtracted from the 82 beam during sample or standard measurements to correct for  $^{82}\text{Kr}$  contribution on  $^{82}\text{Se}$ . The potential gas-based, bromine hydride interference  $^{81}\text{BrH}$  on mass 82 is taken into account through sample standard bracketing.

The contribution of  $^{40}\text{Ar}^{40}\text{Ar}$  at  $m/z = 80$  is then

$$^{40}\text{Ar}^{40}\text{Ar} = I(80) - ^{80}\text{Se} - ^{80}\text{Kr} \quad (4)$$

with  $I(80)$  being the measured intensity at  $m/z = 80$  and  $^{80}\text{Kr}$  calculated using the OPZ  $^{83}\text{Kr}$  and Kr natural abundances. The potential gas-based, bromine hydride interference  $^{79}\text{BrH}$  on mass 81 is taken into account through sample standard bracketing. The potential polyatomic  $^{40}\text{Ar}^{40}\text{Ca}$  interference on mass 80 is deemed negligible, as is no Ca in the pure Se standards used in this study, and for natural samples, the Se chemistry processing should remove any calcium.<sup>34,49</sup>

The amount of  $^{40}\text{Ar}^{40}\text{Ar}$  is determined throughout the run for each integration. The contributions of other argon dimers at mass 76 ( $^{36}\text{Ar}^{40}\text{Ar}$ ;  $^{38}\text{Ar}^{38}\text{Ar}$ ) and 78 ( $^{38}\text{Ar}^{40}\text{Ar}$ ) are deduced from

**Table 2** Interferences and correction method for Se isotope composition measurement. See main text for a detailed explanation of the corrections used. OPZ = on peak zero; HG = hydride generation; SSB = sample standard bracketing

Cup	Measured mass	Se isotopes	Other species and interferences	Correction method
L4	73		$^{73}\text{Ge}$	Used to correct $^{74,76}\text{Ge}$
L3	74	$^{74}\text{Se}$	$^{74}\text{Ge}$	Manual, using $^{73}\text{Ge}$
L2	75		$^{75}\text{As}$ ; $^{75}(\text{SeH})$ ; $^{75}(\text{ArCl})$	Used to correct $^{76}(\text{AsH})$
L1	76	$^{76}\text{Se}$	$^{76}(\text{ArAr})$ ; $^{76}\text{Ge}$ ; $^{76}(\text{AsH})$	Manual, using: $^{80}(\text{ArAr})$ ; $^{73}\text{Ge}$ ; $^{75}\text{As}$ + HG rate
C	77	$^{77}\text{Se}$	$^{77}(\text{SeH})$ ; $^{77}(\text{ArArH})$ ; $^{77}(\text{ArCl})$	Manual, using: $^{76}\text{Se}$ + HG rate; and SSB
H1	78	$^{78}\text{Se}$	$^{78}(\text{ArAr})$ ; $^{78}(\text{SeH})$ ; $^{78}\text{Kr}$	Manual, using: $^{80}(\text{ArAr})$ ; $^{77}\text{Se}$ + HG rate; OPZ on mass 83 – $^{83}\text{Kr}$
H2	80	$^{80}\text{Se}$	$^{80}(\text{ArAr})$ ; $^{80}\text{Kr}$ ; $^{80}(\text{BrH})$	Used to correct Ar dimers; manual, using: OPZ on mass 83 – $^{83}\text{Kr}$ ; SSB
H3	82	$^{82}\text{Se}$	$^{82}\text{Kr}$ ; $^{82}(\text{BrH})$	Manual, using: OPZ on mass 83 – $^{83}\text{Kr}$ ; SSB
H4	83		$^{83}(\text{SeH})$ ; $^{83}\text{Kr}$	Used to assess HG rate; used to correct $^{78,80,82}\text{Kr}$ during OPZ

the  $^{40}\text{Ar}^{40}\text{Ar}$  signal using the natural abundances of 76 and 78 argon dimers – 0.006636 and 0.001257 respectively.<sup>34,55</sup> These contributions are then subtracted from the intensities at mass 76 and 78 (Fig. 2, purple path, argide correction arrows). These *in situ* argide interference corrections greatly reduce the need for long on-peak zero (OPZ, or baseline) measurements and extended wash-out times (of up to one hour<sup>33</sup>), improving sample throughput and reducing reagent consumption.

**Germanium correction.** Naturally present Ge present in samples and incompletely separated from Se in column chemistry can also form hydrides ( $\text{GeH}_4$ ) during the hydride generation process. Germanium possesses 5 stable isotopes –  $^{70}\text{Ge}$ ,  $^{72}\text{Ge}$ ,  $^{73}\text{Ge}$ ,  $^{74}\text{Ge}$  and  $^{76}\text{Ge}$  – two of which –  $^{74}\text{Ge}$  and  $^{76}\text{Ge}$  – create isobaric interferences on mass 74 and mass 76 for the measurement of Se isotopes. Germanium corrections were performed using beam intensity at mass 73 (see Table 2 and Fig. 2). As the cup configuration we used for Se isotope determination does not allow the simultaneous measurement of multiple germanium isotopes, mass bias correction could not be carried out independently for Ge and Se isotopes. Consequently, Ge and Se were assumed to have similar instrumental mass bias and a single instrumental fractionation factor ( $\beta$ ) was used in conjunction with the known natural abundances of Ge isotopes (IUPAC<sup>54</sup>) to calculate the contribution of Ge on mass 74 and mass 76 (eqn (5)):

$${}^{7X}\text{Ge} = {}^{73}\text{Ge} \left( \frac{{}^{7X}\text{Ge}}{{}^{73}\text{Ge}} \right) e^{\beta p^{\text{Ge}}} \quad (5)$$

where  $X = 4$  or  $6$  and  $p^{\text{Ge}} = \ln \frac{\text{mass}({}^{7X}\text{Ge})}{\text{mass}({}^{73}\text{Ge})}$ .

**Hydride corrections.** Hydrides of isotopes of selenium and other impurities still present in samples after column chromatography will all enter the analyser part of the mass spectrometer and interfere on mass ( $N + 1$ ). Previous studies have shown that germanium can form hydrides in the hydride generator at a similar rate as selenium.<sup>33,34</sup> Hydrides of  $^{73}\text{Ge}$  and  $^{76}\text{Ge}$  would be produced at mass 74 and 77, respectively, and interfere with Se measurements. However, given the low Ge contents of post-Se purification chemistry samples, the contribution of Ge hydrides at mass 74 ( $^{73}\text{GeH}$ ) and 77 ( $^{76}\text{GeH}$ ) is negligible and, as shown in previous studies, no GeH correction in purified samples is needed.<sup>33,34</sup> However, the hydrides  $^{76}\text{SeH}$  and  $^{77}\text{SeH}$  directly interfere on Se isotope masses 77 and 78 and must still be accounted for. The hydride generation rate ( $\text{HG}_{\text{rate}}$ ) is estimated by measuring  $^{82}\text{SeH}$  on mass 83 (see Table 2) and using the calculated intensity of  $^{82}\text{Se}_{\text{corr}}$  (eqn (3)), as defined in the following equation:

$$\text{HG}_{\text{rate}} = \frac{{}^{82}\text{SeH}}{{}^{82}\text{Se}_{\text{corr}}} \quad (6)$$

Typically,  $10^{-4} < \text{HG}_{\text{rate}} < 5 \times 10^{-4}$  and is very stable throughout one mass spectrometer session. The hydride generation rate is assumed to be equal for all selenium isotopes

and  $\text{HG}_{\text{rate}}$  is used to correct for the contribution of  $^{76}\text{SeH}$  and  $^{77}\text{SeH}$  on  $^{77}\text{Se}$  and  $^{78}\text{Se}$  signals respectively (see Fig. 2, green path, hydride correction path):

$${}^{7X}\text{SeH} = {}^{7X}\text{Se} \times \text{HG}_{\text{rate}} \quad (7)$$

with  $X = 6$  or  $7$ .

Argon dimers, germanium and arsenic can also form hydrides that will interfere with Se isotopes. Argon dimers of mass 76 ( $^{38}\text{Ar}^{38}\text{Ar}$  and  $^{40}\text{Ar}^{36}\text{Ar}$ ) form hydrides that interfere on mass 77. The hydride generation rate for argon dimers is different from that of the selenium hydride  $\text{HG}_{\text{rate}}$ , as experimentally demonstrated by Pogge von Strandmann *et al.*, 2014,<sup>33</sup> which is expected as ArAr is a molecule while Se is an atom. It is therefore not possible to correct for the contribution of ArArH on mass 77 using the hydride generation rate estimated with the Se ion beam. However, the contribution of ArArH can be corrected in a straightforward manner using sample standard bracketing, as the argon dimer generation rate is similar in samples and standards of equal Se concentration ( $\pm 5\%$ ).

Although  $^{75}\text{As}$  does not directly interfere on any Se isotope masses,  $^{75}\text{As}$  can form  $^{75}\text{AsH}$  hydrides if present in the analyte, thus interfering on  $^{76}\text{Se}$ . To correct for the arsenic hydride contribution on mass 76, we assume that the hydride generation rate for  $^{75}\text{AsH}$  is similar to that of selenium isotopes (see Fig. 2, green path, hydride correction path). Mass 75 is monitored throughout the measurement to obtain the  $^{75}\text{As}$  signal. The  $^{75}\text{AsH}$  contribution on mass 76 is therefore

$${}^{75}\text{AsH} = {}^{75}\text{As}_{\text{corr}} \text{HG}_{\text{rate}} = {}^{75}\text{As} \frac{{}^{82}\text{SeH}}{{}^{82}\text{Se}_{\text{corr}}} \quad (8)$$

with  ${}^{75}\text{As}_{\text{corr}}$ :  $^{75}\text{As}$  corrected for  $^{40}\text{Ar}^{35}\text{Cl}$  using the on peak zero measurement.

## 4. Results and discussion

### 4.1. Internal precision, reproducibility and accuracy of double spike measurements

Internal precision on  $\delta^{82/78}\text{Se}$  for a single analysis of one block of 80 cycles, with 4 seconds integration time, typically ranges from 0.010 to 0.025‰ (95% c.i., 2 s.e.), as shown in Fig. 3, which compares well with the predicted internal errors for a similar beam intensity. Larger errors reported for some measurements are linked to short-term instability of the argon dimer and/or hydride generation rates (see Fig. 3). Once errors on bracketing standards are propagated, internal errors on bracketed sample data typically range 0.014 to 0.033‰ (95% c.i.). Our estimates of long-term reproducibility are discussed in further detail below.

### 4.2. NIST SRM 3149 scaling to Merck Se

In this study, we report the isotopic composition of the international Se standard reference material NIST SRM 3149 relative to the same MERCK Se solution first measured by Rouxel *et al.*, 2002,<sup>6</sup> and then calibrated by Carignan and Wen in 2007.<sup>35</sup> We measured the MERCK Se solution 93 times during 15 different

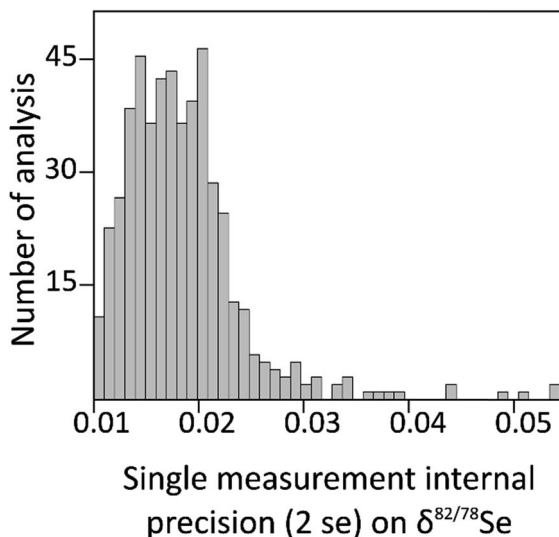


Fig. 3 Internal precision on  $\delta^{82/78}\text{Se}$  for all single measurements included in this study (2 s.e.), for 1 block of 80 cycles, with 4 seconds integration time. Errors typically range from ca. 0.01 to 0.025‰ (95% c.i.) although some larger errors can occur when the mass spectrometer is unstable. Once errors on bracketing standards are taken into account, errors on sample data typically range from 0.014 to 0.033‰ (95% c.i.).

analytical sessions, spanning from June 2014 to January 2016, from  $n = 4$  to  $n = 9$  times in each session. The results are presented in Fig. 4. During individual analytical sessions, the isotopic composition of the Se MERCK solution relative to Se NIST SRM-3149 was between  $-0.958$  and  $-1.027$ ‰ with a 2 s.d. error ranging from 0.015‰ for the best session ( $n = 6$ ) to 0.030‰ for the less reproducible one ( $n = 7$ ). We obtained an overall  $\delta^{82/78}\text{Se}$  composition for the MERCK Se solution of  $-0.988 \pm 0.034$ ‰ (2 s.d. from the weighed means of analytical sessions, total

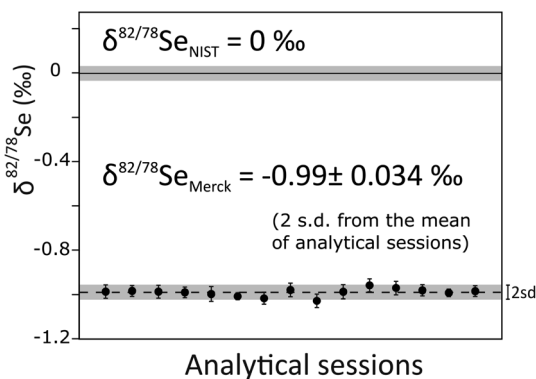


Fig. 4 Merck Se solution calibration to Se NIST SRM-3149. Results obtained during all the analytical sessions. Error bars are 2 times the standard deviation for results obtained during individual sessions ( $n = 4$  to 9). The grey area corresponds to the long-term external reproducibility ( $\pm 2$  s.d. = 0.040‰,  $n = 93$ ). The value of Merck Se relative to Se NIST SRM 3149 is  $\delta^{82/78}\text{Se}_{\text{Merck}} = -0.99 \pm 0.034$ ‰ (2 s.d., from the mean of analytical sessions), which is in perfect agreement with previous calibration by Carignan and Wen, 2007 ( $\delta^{82/78}\text{Se}_{\text{Merck}} = -1.03 \pm 0.20$ ‰, Carignan and Wen, 2007).

number of analyses  $n = 93$ ) relative to the Se NIST SRM-3149 international standard, which is well within analytical precision of Carignan and Wen's calibrated value of  $-1.03 \pm 0.20$ ‰.<sup>35</sup> Taking into account all measurements ( $n = 93$ ), Se MERCK yields a value of  $\delta^{82/78}\text{Se} = -0.989 \pm 0.040$ ‰ (2 s.d.,  $n = 93$ ), which is the long-term average standard reproducibility obtained in this study.

Our protocol has allowed us to improve on the reproducibility of Se isotope measurements, as reported in recent published studies, such as in Kurzawa *et al.*, 2017 (2 s.d. = 0.13‰ on  $\delta^{82/78}\text{Se}$  for repeated measurements of the MH-495 Se standard,  $n = 100$  (ref. 29)) or in Chang *et al.*, 2017 (2 s.d. = 0.07‰ on  $\delta^{82/78}\text{Se}$  for repeated measurements of Merck lot HC44698550 and lot HC44697996 Se standards,  $n = 24$  and 10 respectively<sup>36</sup>). However, direct comparison of these methods is difficult as these different studies involved Se isotope analyses carried out on solutions of different Se concentrations and hence beam intensities. For example, in Kurzawa *et al.*, 2017, measurements were performed at 15 ppb Se solution, while the measurements in our study involved solutions of 50 ppb Se. The effect of counting statistics related to differences in concentration can be calculated, which gives us access to an estimate of our potential reproducibility at 15 ppb of 0.073‰, which is roughly half of that obtained by Kurzawa *et al.*, 2017. As we have accounted for Johnson noise, this difference must be related to different hydride and argon dimer correction strategies.<sup>29</sup> As for Chang *et al.*, 2017, it is unclear at what concentration they performed their measurements, therefore no direct comparison should be drawn.<sup>56</sup>

#### 4.3. Robustness of the method

**Correction of isobaric interferences related to germanium and arsenic.** The accuracy of the Ge corrections used in our

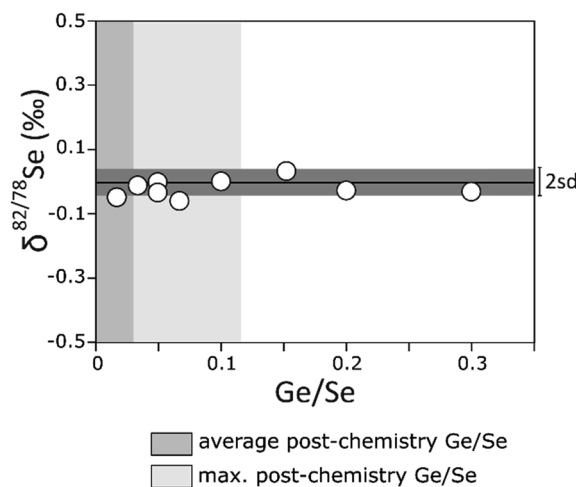


Fig. 5 Ge doping experiments on NIST SRM-3149 and its effect on the Se isotope composition measurement. The solid black line represents 0‰ and the dark grey area corresponds to the long-term external reproducibility ( $\pm 2$  s.d. = 0.040‰). In a single analysis ( $n = 80$ ), the internal error for  $\delta^{82/78}\text{Se}$  is 0.010 < 2 s.e. < 0.025‰, which is smaller than the marker's size. The light grey area represents the average post-TCF chemistry Ge/Se ratio, and the medium grey area represents the maximum post-TCF chemistry Ge/Se ratio (Pogge von Strandmann *et al.*, 2014).

protocol was tested by measuring multiple Ge-doped selenium solutions. The results are shown in Fig. 5. Solutions with a Ge/Se ratio of up to 0.3 were tested, which represents  $\sim 3$  times the maximum post-TCF (thiol cotton fibre) chemistry Ge/Se ratio in detrital sediments.<sup>33</sup> Up to a post-TCF chemistry Ge/Se ratio of 0.3, our corrected measurements are within the long-term external reproducibility of 0.034‰ of un-doped standards (2 s.d.; see Fig. 5). For samples highly enriched in germanium such as some hydrothermal veins and deposits,<sup>57</sup> TCF chemistry might produce Ge/Se ratios greater than 1, in which case the monitoring of a second Ge mass (*e.g.*  $^{72}\text{Ge}$ ) might prove useful to independently monitor Ge mass bias, rather than assuming that it is identical to that of Se. Another way to reduce the Ge/Se ratio in measured samples is to use the anion/cation-exchange resin-based Se purification and extraction protocol recently developed by Kurzawa *et al.* (Kurzawa *et al.*, 2017, method developed and adapted after Fehr *et al.*, 2004, and Wang *et al.*, 2013), which gives better and more robust Se purification than the TCF protocol.<sup>29,58,59</sup>

The accuracy of the arsenic hydride correction was tested by measuring several As-doped NIST SRM-3149 selenium standard solutions, with As/Se ranging from 0.02 to 0.5. The results are plotted in Fig. 6. For  $0 < \text{As/Se} < 0.3$ , all corrected measurements yield the correct Se NIST SRM-3149 isotopic composition within error with our long-term external reproducibility ( $\pm 2$  s.d. = 0.034‰). Average post-TCF chemistry As/Se ratios are typically  $< 0.15$  for detrital sediments, as shown by Pogge von Strandmann *et al.* in their 2014 study.<sup>33</sup> The maximum post-TCF chemistry As/Se ratio obtained by Pogge von Strandmann *et al.* is 0.3,<sup>33</sup> meaning that our arsenic hydride correction is adequate for TCF chemistry-processed samples with similar

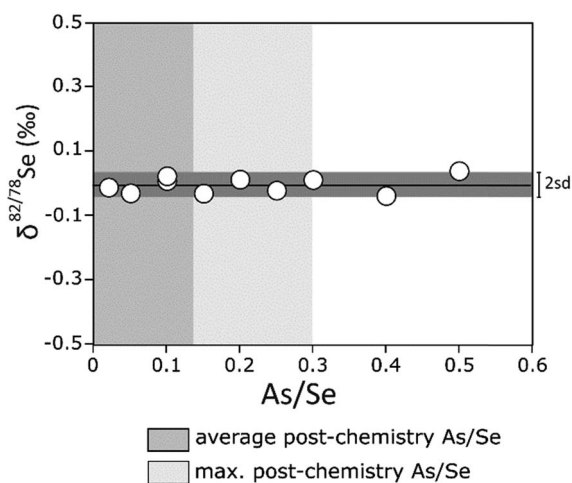


Fig. 6 As doping experiments on NIST SRM-3149 and effect on the Se isotope composition measurement. The solid black line represents 0‰ and the dark grey area corresponds to the long-term external reproducibility ( $\pm 2$  s.d. = 0.040‰). On a single analysis ( $n = 80$ ), the internal error for  $\delta^{82/78}\text{Se}$  is  $0.010 < 2 \text{ s.e.} < 0.025\text{‰}$ , which is smaller than the marker's size. The light grey area represents the average post-TCF chemistry As/Se ratio, and the medium grey area represents the maximum post-TCF chemistry As/Se ratio (Pogge von Strandmann *et al.*, 2014).

matrices. Prior to using this correction on Se samples processed *via* anion/cation exchange resin column chemistry,<sup>29,58,59</sup> further tests on the final As/Se ratio should be performed.

**Effect of non-ideal spike/sample mixtures.** The developed  $^{76}\text{Se}$ – $^{78}\text{Se}$  double spike is designed to give the best error for a 50% sample–50% double spike mixture (see Fig. 1). The double spike fraction,  $f_{\text{spike}}$ , is equal to 0.5 for this ideal mixture (see Fig. 7). Achieving the perfect selenium sample to spike ratio to perform Se isotope measurements is not trivial, for two major reasons. The first issue is that it is difficult to precisely measure Se concentrations in geological samples, because (i) terrestrial and extra-terrestrial rocks, with the exception of some Se-rich sediments such as shales, contain a very low amount of selenium (*e.g.* from 1 to 100 ppb in peridotites, from 1 to 200 ppb in igneous rocks, from 3 to 27 ppm in chondrites;<sup>22,26–28,50,60</sup>) (ii) as a volatile element, Se can be lost during sample preparation;<sup>26,30,31,34</sup> and (iii) issues related to plasma source mass spectrometry similar to those discussed in previous sections – in particular the low Se ionization and argon dimers.<sup>26,27</sup>

The other major issue is directly related to the low abundance of selenium in geological samples: precisely measuring one sample's concentration may simply require too much of the sample concerned. This is particularly limiting when dealing with precious and unique samples such as meteorites (*e.g.* Murchison, 12.2 ppm Se<sup>22</sup>) or rare and old fossils. In this context, it is of primary importance to assess the effect of non-ideal spike to sample mixtures on the measurement of Se isotopes and to determine how tolerant our  $^{76}\text{Se}$ – $^{78}\text{Se}$  double spike is toward such mixing uncertainties. In order to test this effect, several non-ideal spike to Se NIST SRM-3149 (sample) mixtures were measured, with the double spike fraction  $f_{\text{spike}}$  ranging from 0.2 (mixture: 20%  $^{76}\text{Se}$ – $^{78}\text{Se}$  double spike + 80% sample of Se NIST SRM-3149) to 0.8 (mixture: 80%  $^{76}\text{Se}$ – $^{78}\text{Se}$  double spike + 20% sample of Se NIST SRM-3149). The results

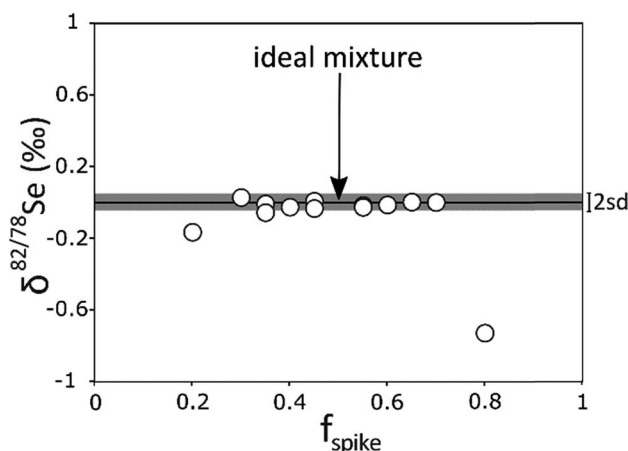


Fig. 7 Effect of variably spiking Se NIST SRM-3149 on Se isotope measurements using a  $^{76}\text{Se}$ – $^{78}\text{Se}$  double spike. The ideal mixture is 50% sample, 50% spike ( $f_{\text{spike}} = 0.5$ ). The solid black line represents 0‰ and the dark grey area corresponds to the long-term external reproducibility ( $\pm 2$  s.d. = 0.040‰). In a single analysis ( $n = 80$ ), the internal error for  $\delta^{82/78}\text{Se}$  is  $0.010 < 2 \text{ s.e.} < 0.025\text{‰}$ , which is smaller than the marker's size.

are shown in Fig. 7. For  $0.3 < f_{\text{spike}} < 0.7$ , the Se NIST SRM-3149  $\delta^{82/78}\text{Se}$  values are within the long-term external reproducibility of  $0.034\text{‰}$  (2 s.d.) and indistinguishable from the ideal 50% double spike–50% sample mixture. Outside this  $f_{\text{spike}}$  range, the measured values should be discarded, as the offset from the right value increases quickly ( $0.18\text{‰}$  for  $f_{\text{spike}} = 0.2$ ;  $0.71\text{‰}$  for  $f_{\text{spike}} = 0.8$ ; see Fig. 7).

**Effect of standard/sample concentration mismatch.** Our method combines the use of a  $^{76}\text{Se}$ – $^{78}\text{Se}$  double spike and sample-standard bracketing (SSB), by bracketing each sample with two measurements of a double-spiked NIST SRM-3149 Se pure standard. The use of SSB along with the double spike allows us to correct for small variations in gas-based interferences and hydride generation (e.g. for bromine hydrides  $^{79}\text{BrH}$  and  $^{81}\text{BrH}$  on masses 80 and 82 respectively or argon chloride molecules,  $\text{ArCl}$ , on mass 77; see Table 2) which are not directly accounted for in our interference corrections and hence double-

spike deconvolution. As for isotope measurement methods relying purely on SSB (e.g.  $\text{Zn}$ , $^{61,62}\text{Fe}$  and  $\text{Cu}^{63}$ ), measured samples and standards should share the same concentration. We have tested the effect of sample/standard concentration mismatch on the quality and reproducibility of our Se isotope measurements (see Fig. 8). Samples with a concentration that differs from the standard concentration by systematic amounts were measured and bracketed with a double-spiked NIST SRM-3149 Se pure standard of concentration 125 ppb. Concentration mismatch has a large effect on  $\delta^{82/78}\text{Se}$  measurements. A concentration mismatch of  $\pm 10\%$  can generate an error on the  $\delta^{82/78}\text{Se}$  value of 0.1 to  $0.2\text{‰}$  (see Fig. 8), which is considerably greater than our long-term reproducibility (2 s.d. =  $0.034\text{‰}$ ) calculated for sample/standards of equal concentration. A concentration mismatch greater than 45% will impact the  $\delta^{82/78}\text{Se}$  value by more than  $1\text{‰}$  (Fig. 8). Our tests show that concentration matching between the samples and the standard is the most critical parameter to optimise in these measurements. Sample dilution before measurements on a MC-ICPMS therefore needs to be done extremely carefully, and in the case of a concentration mismatch larger than 5%, we recommend discarding the data and performing the measurement again.

## 5. Conclusions

This study presents a methodology to precisely measure selenium isotopes, based on the development of a  $^{76}\text{Se}$ – $^{78}\text{Se}$  double-spike. Our double spike was designed to minimise the error in Se isotope measurements, and while our choice of  $^{76}\text{Se}$  and  $^{78}\text{Se}$  as spiked elements is unusual – as both these isotopes show interferences with argon dimers – we can demonstrate that this issue can be addressed with systematic interference corrections made prior to spike deconvolution. In particular, the monitoring of argide formation on mass 80 and the subtraction of argon dimer contribution on mass 76 and 78 in each integration, during the measurement, have proven essential. Our setting for hydride generation coupled to a ThermoFisher™ Scientific Neptune Plus™ MC-ICPMS produces an overall sensitivity of over 1000 V per ppm of Se. By combining this improved sensitivity with our double spike and integration-by-integration argon dimer correction, our method requires 25 ng of natural Se to perform one measurement, and we obtain a long-term external reproducibility of  $0.040\text{‰}$  (2 s.d.,  $n = 93$ ). This method should enable the measurement of the Se isotope composition of a wide array of geological samples, thus firmly establishing Se stable isotopes as a novel addition to the geochemist toolbox.

## Conflicts of interest

There are no conflicts of interest to declare.

## Acknowledgements

This work was supported by ThermoScientific, an ERC Starting Grant (HabitablePlanet; 306655), and two NERC Consortium

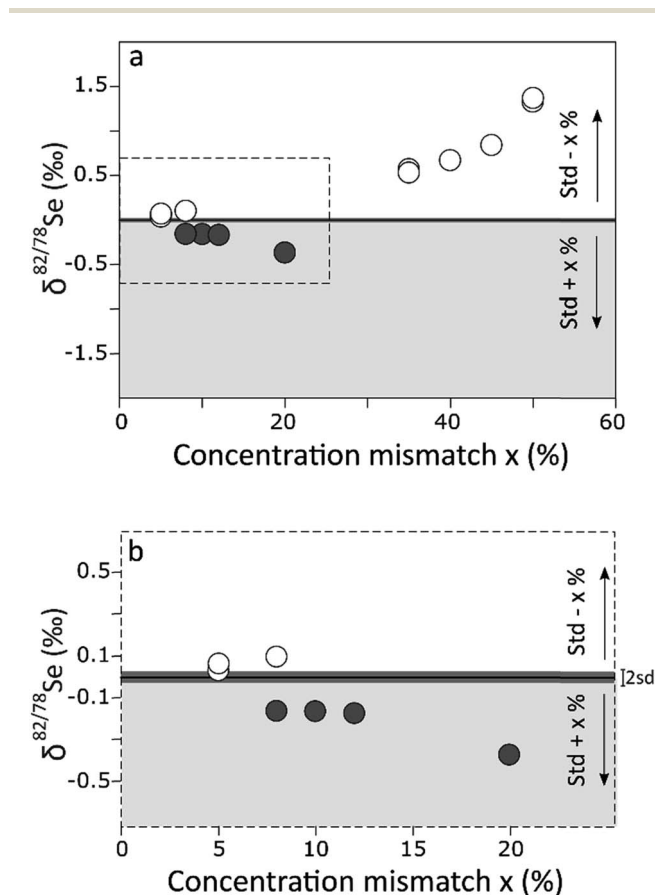


Fig. 8 Effect of sample to standard concentration mismatch on Se isotope measurements. (a) Effect of sample–standard concentration mismatch during SSB measurements on the sample  $\delta^{82/78}\text{Se}$ . (b) Magnification of the dashed area from figure (a). In both (a) and (b), the solid black line represents  $0\text{‰}$  and the dark grey area corresponds to the long-term external reproducibility ( $\pm 2$  s.d. =  $0.040\text{‰}$ ). In a single analysis ( $n = 80$ ), the internal error for  $\delta^{82/78}\text{Se}$  is  $0.010 < 2$  s.e.  $< 0.025\text{‰}$ , which is smaller than the marker's size. White area and white markers: the sample has a lower concentration than the standard. Light grey area and grey markers: the sample has a greater concentration than the standard.

Grants (“Deep Volatiles”, NE/M0003/1 and “Tellurium and Selenium Cycling and Supply (TeAsE)” NE/M010848/1) awarded to HW. HW and MLP also acknowledge salary support from a NERC Advanced Fellowship (NE/F014295/2) and a MSCA Individual Fellowship (SPECADIS, 794825), respectively. We thank Philip Pogge von Strandmann for helpful discussions and tips to set up the measurements, and Kathrin Schilling and Tom Johnson for their help and advice throughout the project. We thank the three anonymous reviewers for their constructive comments which helped improve the manuscript.

## References

- 1 A. Galy, N. S. Belshaw, L. Halicz and R. K. O’Nions, *Int. J. Mass Spectrom.*, 2001, **208**, 89–98.
- 2 M.-A. Millet and N. Dauphas, *J. Anal. At. Spectrom.*, 2014, **29**, 1444.
- 3 C. Siebert, T. F. Nägler and J. D. Kramers, *Geochem., Geophys., Geosyst.*, 2001, **2**, 159–171.
- 4 R. Schoenberg, S. Zink, M. Staubwasser and F. von Blanckenburg, *Chem. Geol.*, 2008, **249**, 294–306.
- 5 N. Dauphas and O. Rouxel, *Mass Spectrom. Rev.*, 2006, **25**, 515–550.
- 6 O. Rouxel, J. Ludden, J. Carignan, L. Marin and Y. Fouquet, *Geochim. Cosmochim. Acta*, 2002, **66**, 3191–3199.
- 7 M. A. Kipp, E. E. Stüeken, A. Bekker and R. Buick, *Proc. Natl. Acad. Sci. U. S. A.*, 2017, **114**, 875–880.
- 8 E. E. Stüeken, R. Buick and A. D. Anbar, *Geology*, 2015, **43**, 259–262.
- 9 H. Wen and J. Carignan, *Geochim. Cosmochim. Acta*, 2011, **75**, 1411–1427.
- 10 H. Wen, J. Carignan, X. Chu, H. Fan, C. Cloquet, J. Huang, Y. Zhang and H. Chang, *Chem. Geol.*, 2014, **390**, 164–172.
- 11 E. E. Stüeken, R. Buick, A. Bekker, D. Catling, J. Foriel, B. M. Guy, L. C. Kah, H. G. Machel, I. P. Montañez and S. W. Poulton, *Geochim. Cosmochim. Acta*, 2015, **162**, 109–125.
- 12 E. E. Stüeken, *Rev. Mineral. Geochem.*, 2017, **82**, 657–682.
- 13 S. König, B. Eickmann, T. Zack, A. Yierpan, M. Wille, H. Taubald and R. Schoenberg, *Geochim. Cosmochim. Acta*, 2019, **244**, 24–39.
- 14 P. A. E. Pogge von Strandmann, E. E. Stüeken, T. Elliott, S. W. Poulton, C. M. Dehler, D. E. Canfield and D. C. Catling, *Nat. Commun.*, 2015, **6**, 10157.
- 15 K. Schilling, T. M. Johnson and W. Wilcke, *Chem. Geol.*, 2013, **352**, 101–107.
- 16 K. Schilling, T. M. Johnson, K. S. Dhillon and P. R. D. Mason, *Environ. Sci. Technol.*, 2015, **49**, 9690–9698.
- 17 A. Basu, K. Schilling, S. T. Brown, T. M. Johnson, J. N. Christensen, M. Hartmann, P. W. Reimus, J. M. Heikoop, G. Woldegabriel and D. J. DePaolo, *Environ. Sci. Technol.*, 2016, **50**, 10833–10842.
- 18 K. Schilling, T. M. Johnson and W. Wilcke, *Soil Sci. Soc. Am. J.*, 2011, **75**, 1354.
- 19 T. M. Johnson, M. J. Herbel, T. D. Bullen and P. T. Zawislanski, *Geochim. Cosmochim. Acta*, 1999, **63**, 2775–2783.
- 20 M. J. Herbel, T. M. Johnson, R. S. Oremland and T. D. Bullen, *Geochim. Cosmochim. Acta*, 2000, **64**, 3701–3709.
- 21 T. Kurzawa, S. König, J. C. Alt, A. Yierpan and R. Schoenberg, *Chem. Geol.*, 2019, **513**, 239–249.
- 22 J. Labidi, S. König, T. Kurzawa, A. Yierpan and R. Schoenberg, *Earth Planet. Sci. Lett.*, 2018, **481**, 212–222.
- 23 H. Vollstaedt, K. Mezger and I. Leya, *Earth Planet. Sci. Lett.*, 2016, **450**, 372–380.
- 24 A. Yierpan, S. König, J. Labidi and R. Schoenberg, *Geochim. Cosmochim. Acta*, 2019, **249**, 199–224.
- 25 M. I. Varas-Reus, S. König, A. Yierpan, J.-P. Lorand and R. Schoenberg, *Nat. Geosci.*, 2019, **12**, 779–782.
- 26 J.-P. Lorand and O. Alard, *Chem. Geol.*, 2010, **278**, 120–130.
- 27 S. König, A. Luguët, J.-P. Lorand, F. Wombacher and M. Lissner, *Geochim. Cosmochim. Acta*, 2012, **86**, 354–366.
- 28 J.-P. Lorand, O. Alard, A. Luguët and R. R. Keays, *Geochim. Cosmochim. Acta*, 2003, **67**, 4137–4151.
- 29 T. Kurzawa, S. König, J. Labidi, A. Yierpan and R. Schoenberg, *Chem. Geol.*, 2017, **466**, 219–228.
- 30 K. Schilling, T. M. Johnson and P. R. D. Mason, *Chem. Geol.*, 2014, **381**, 125–130.
- 31 A. Yierpan, S. König, J. Labidi, T. Kurzawa, M. G. Babechuk and R. Schoenberg, *Geochem., Geophys., Geosyst.*, 2018, **19**, 516–533.
- 32 H. Vollstaedt, K. Mezger, T. Nägler, I. Leya and A. Trinquier, *Int. J. Mass Spectrom.*, 2016, **401**, 55–63.
- 33 P. A. E. Pogge von Strandmann, C. D. Coath, D. C. Catling, S. W. Poulton and T. Elliott, *J. Anal. At. Spectrom.*, 2014, **29**, 1648–1659.
- 34 E. E. Stüeken, J. Foriel, B. K. Nelson, R. Buick and D. C. Catling, *J. Anal. At. Spectrom.*, 2013, **28**, 1734.
- 35 J. Carignan and H. Wen, *Chem. Geol.*, 2007, **242**, 347–350.
- 36 F. Albarede and B. Beard, *Rev. Mineral. Geochem.*, 2004, **55**, 113–152.
- 37 B. Hamelin, G. Manhes, F. Albarede and C. J. Allègre, *Geochim. Cosmochim. Acta*, 1985, **49**, 173–182.
- 38 M. H. Dodson, *J. Sci. Instrum.*, 1963, **40**, 289–295.
- 39 M. H. Dodson, *Geochim. Cosmochim. Acta*, 1970, **34**, 1241–1244.
- 40 J. F. Rudge, B. C. Reynolds and B. Bourdon, *Chem. Geol.*, 2009, **265**, 420–431.
- 41 M. H. Dodson, *J. Phys. E: Sci. Instrum.*, 1969, **2**, 490–498.
- 42 S. G. John, *J. Anal. At. Spectrom.*, 2012, **27**, 2123.
- 43 F. Kurzweil, M. Wille, N. Gantert, N. J. Beukes and R. Schoenberg, *Earth Planet. Sci. Lett.*, 2016, **452**, 69–78.
- 44 G. Albut, M. G. Babechuk, I. C. Kleinhanns, M. Bengler, N. J. Beukes, B. Steinhilber, A. J. B. Smith, S. J. Kruger and R. Schoenberg, *Geochim. Cosmochim. Acta*, 2018, **228**, 157–189.
- 45 M.-A. Millet, J. A. Baker and C. E. Payne, *Chem. Geol.*, 2012, **304–305**, 18–25.
- 46 A. J. McCoy-West, M.-A. Millet and K. W. Burton, *Earth Planet. Sci. Lett.*, 2017, **480**, 121–132.
- 47 J. A. M. Nanne, M.-A. Millet, K. W. Burton, C. W. Dale, G. M. Nowell and H. M. Williams, *J. Anal. At. Spectrom.*, 2017, **32**, 749–765.
- 48 S. J. G. Galer, *Chem. Geol.*, 1999, **157**, 255–274.

- 49 T. Kurzawa, S. König, J. Labidi, A. Yierpan and R. Schoenberg, *Chem. Geol.*, 2017, **466**, 219–228.
- 50 J.-M. Zhu, T. M. Johnson, S. K. Clark, X.-K. Zhu and X.-L. Wang, *Geochim. Cosmochim. Acta*, 2014, **126**, 228–249.
- 51 J. Wang, T. Ren, H. Lu, T. Zhou and M. Zhao, *Int. J. Mass Spectrom.*, 2011, **308**, 65–70.
- 52 S. K. Clark and T. M. Johnson, *Environ. Sci. Technol.*, 2008, **42**, 7850–7855.
- 53 N. Elwaer and H. Hintelmann, *J. Anal. At. Spectrom.*, 2008, **23**, 733.
- 54 J. Meija, T. B. Coplen, M. Berglund, W. A. Brand, P. De Bièvre, M. Gröning, N. E. Holden, J. Irrgeher, R. D. Loss, T. Walczyk and T. Prohaska, *Pure Appl. Chem.*, 2016, **88**, 293.
- 55 J.-Y. Lee, K. Marti, J. P. Severinghaus, K. Kawamura, H.-S. Yoo, J. B. Lee and J. S. Kim, *Geochim. Cosmochim. Acta*, 2006, **70**, 4507–4512.
- 56 Y. Chang, J. Zhang, J.-Q. Qu and Y. Xue, *Chem. Geol.*, 2017, **471**, 65–73.
- 57 F. Sahlström, A. Arribas, P. Dirks, I. Corral and Z. Chang, *Minerals*, 2017, **7**, 213.
- 58 M. A. Fehr, M. Rehkämper and A. N. Halliday, *Int. J. Mass Spectrom.*, 2004, **232**, 83–94.
- 59 Z. Wang and H. Becker, *Nature*, 2013, **499**, 328.
- 60 Y. Tamari, H. Ogawa, Y. Fukumoto, H. Tsuji and Y. Kusaka, *Bull. Chem. Soc. Jpn.*, 1990, **63**, 2631–2638.
- 61 M.-L. Pons, B. Debret, P. Bouilhol, A. Delacour and H. Williams, *Nat. Commun.*, 2016, **7**, 13794.
- 62 C. N. Maréchal, P. Télouk and F. Albarède, *Chem. Geol.*, 1999, **156**, 251–273.
- 63 K. Jaouen, M.-L. Pons and V. Balter, *Earth Planet. Sci. Lett.*, 2013, **374**, 164–172.